LA-UR- 02-5975

Approved for public release; distribution is unlimited.

Title: Initial Tests of a Thermoacoutic Space Power Engine

Author(s): Scott Backhaus, MST-10

Submitted to: Space Technology and Applications International Forum

Los Alamos
NATIONAL LABORATORY

Initial Tests of a Thermoacoustic Space Power Engine

Scott Backhaus[1]

[1]*Condensed Matter and Thermal Physics Group, Los Alamos National Laboratory, Los Alamos, NM 87545*

Abstract. Future NASA deep-space missions will require radioisotope-powered electric generators that are just as reliable as current RTGs, but more efficient and of higher specific power (W/kg). Thermoacoustic engines at the ~1-kW scale have converted high-temperature heat into acoustic, or PV, power without moving parts at 30% efficiency. Consisting of only tubes and a few heat exchangers, thermoacoustic engines are low mass and promise to be highly reliable. Coupling a thermoacoustic engine to a low mass, highly reliable and efficient linear alternator will create a heat-driven electric generator suitable for deep-space applications. Conversion efficiency data will be presented on a demonstration thermoacoustic engine designed for the 100-Watt power range.

INTRODUCTION

Thermoacoustic engines are a class of engines that convert high-temperature heat into acoustic, or PV, power without using moving parts. Recent innovations in thermoacoustics have allowed these engines to utilize the more efficient Stirling thermodynamic cycle (Backhaus, 2000). The result has been an increase in thermal-to-PV conversion efficiency from ~21% to 30%. The Thermoacoustic-Stirling Heat Engine (TASHE) that demonstrated 30% efficiency produced ~1kW of PV power.

Future NASA deep-space missions will require highly reliable (>100,000-hour lifetime), high specific power (~10 W/kg), and efficient (13%-25%) thermal-to-electric converters in the 100-W_e power range (Mondt, 2001). These converters will be powered by high-temperature heat from the radioactive decay of ^{238}Pu contained in a General Purpose Heat Source (GPHS). Since a TASHE has no moving parts, it has the promise to be highly reliable, and it has demonstrated high efficiency in the 1-kW power range. By coupling a TASHE to a linear alternator that takes its heritage from flight-proven, high-efficiency linear compressors used in space-based cryocoolers (Tward, 1999), a new type of reliable thermal-to-electric converter will be created.

The critical component in this converter is the TASHE. All past work on TASHEs has been done in the 1-kW range and above. Scaling the TASHE down to the 100-W range, while maintaining its high efficiency, minimizing its mass, and providing easy thermal and mechanical interfaces to the rest of the power system, is critical to the success of this new conversion technology. The next two sections describe the design and recent modifications of a 100-W class demonstration TASHE and conversion efficiency tests using an acoustical resonator as a replacement for a linear alternator

ENGINE DESIGN AND DESCRIPTION

The layout of the demonstration TASHE is shown in Figure 1. Except for a few modifications described below, it is similar to an earlier version (Backhaus 2001). Therefore, only a general description of its components and operation will be given. A detailed description of its components and operation is given in the references (Backhaus 2001, Backhaus 2000). The TASHE is composed of a looped flow path filled with high-pressure helium gas. The loop contains the regenerator, heat exchangers, and other ductwork necessary to force the gas in the regenerator to execute the Stirling cycle (Backhaus, 2000). Prior to the recent modifications in which maintaining low mass was not a considered, the mass of the demonstration TASHE up to the resonator/alternator interface was approximately 900 grams. At this 100-W scale, the TASHE contributes less than 10% of the mass in the 10 W/kg space-power

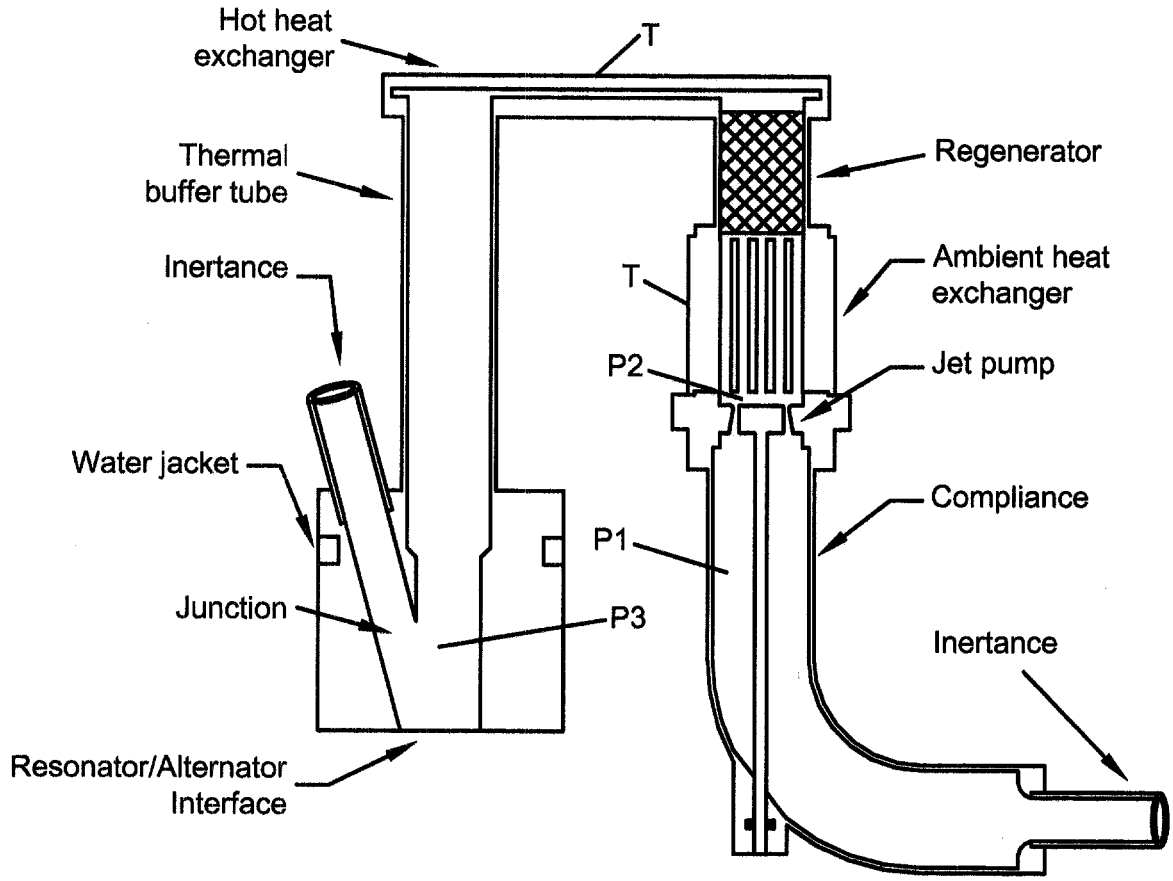

FIGURE 1. Schematic drawing of the TASHE. All parts have circular cross section, *i.e.* tubular, expect the hot heat exchanger, which has a rectangular cross section with the long transverse dimension into the page. For clarity, the compliance is shown rotated 90°. The nickel heater block, cooling water jacket on the ambient heat exchanger, and the flow straighteners in the thermal buffer tube (TBT) are not shown. The TASHE is insulated from the top of the hot heat exchanger to the ambient ends of the TBT and regenerator. For clarity, the compliance is shown rotated 90°. The two inertance tubes are joined by additional tubing of the same diameter. In a flight design, the water jacket and junction between the TBT would be integrated into the alternator so that no extra metal is required to form this geometry. The overall height of the TAHSE is approximately 16cm. Temperature and pressure measurements are made at locations labeled T and P1 through P3 respectively.

system desired by NASA (Mondt, 2001). If designed for a flight system instead of laboratory convenience, much of the instrumentation, bolting flanges, and extraneous metal in the TASHE would be removed and aluminum would be substituted for several of the stainless steel components resulting in additional mass savings.

Since the TASHE has no moving parts, its geometry is very flexible. The design shown in Figure 1 is chosen so that the hot end of the TASHE is flat and exposed on one end. This configuration allows for simple thermal and mechanical interfaces to the GPHS. In principle, solid conduction from the GPHS to the hot heat exchanger could be used to couple the heat into the TASHE. An interface of this type should not require any additional metal to transport the heat to the TASHE or to support the GPHS. This provides an additional mass savings when the converter is integrated with the rest of the power system. With no moving parts in the hot end of the TASHE, creep of the hot end material induced by the high temperatures and high internal pressure will not affect performance due to the loss of a critical tolerance.

The hot heat exchanger is a small gap between two Inconel 625 parallel plates. High-temperature heat enters the system by solid conduction through the top plate (maximum operating metal temperature of 650 °C). In the test, the high-temperature heat is generated by 4 electrically-powered heaters embedded in a nickel block (not shown) soldered to the top surface of the hot heat exchanger. Heat enters the helium working gas as it oscillates along the inner surface of the top plate. Proceeding down the right leg of the loop is the regenerator, which is composed of a

stack of stainless-steel screen housed in an Inconel 625 cylinder. Below the regenerator is the ambient heat exchanger. It is an aluminum cylinder with 48 long holes drilled through. In these laboratory tests, cooling water flowing through a copper water jacket shrunk fit to the aluminum cylinder finally carries the waste heat rejected through this heat exchanger away. The ambient heat exchanger has been lengthened to match the peak-to-peak displacement of the helium gas and, therefore, reduce the temperature difference between the helium and heat exchanger metal.

In the left leg of the loop below the hot heat exchanger is the Inconel 625 thermal buffer tube (TBT). The TBT allows acoustic power to flow away from the hot heat exchanger while thermally isolating the hot end from ambient temperature. Flow straighteners at either end ensure that the flow in the TBT remains thermally stratified. In a previous version (Backhaus 2001), a secondary ambient heat exchanger below the ambient flow straightener confined the temperature gradient to the TBT keeping the alternator/resonator interface from experiencing elevated temperatures. During testing, it was found that simply cooling the outside of the pressure vessel was sufficient. Therefore, the secondary heat exchanger has been removed. This will simplify the ambient end thermal interfaces to the TASHE.

The left and right legs of the TASHE are rejoined by a constant diameter inertance tube that connects to the left leg at the alternator/resonator interface and to the right leg at the compliance. The inertance tube and compliance form an acoustic network that generates pressure and velocity oscillations in the regenerator that drive the gas through the Stirling cycle (Backhaus, 2000). The inertia of the helium gas in the inertance tube can loosely be compared to that of a displacer piston in a free-piston Stirling engine. To reduce minor losses at the junction, the inertance tube and the TBT have been joined with a streamlined 15-degree "wye" instead of a 90-degree "tee". Also, the area of the left leg is reduced after the TBT so that the velocity of the gas coming from the inertance tube and TBT are equal as they join at the alternator/resonator interface. Also, the volume of the compliance has been increased to boost the PV power output, and the geometry of the inertance tube-to-compliance junction has been streamlined.

The final component in the loop is located between the main ambient heat exchanger and the compliance. Called a "jet pump", it is an annular diffuser with the small end facing the main ambient heat exchanger. The area of the small-end opening is adjustable by moving the central plug in the axial direction. The asymmetry of the flow out of the small end creates an adjustable time-averaged pressure drop that generates a steady flow around the TASHE's loop. This flow is used to cancel a parasitic steady flow around the loop generated by acoustic streaming (Gedeon, 1997). Without the action of the jet pump, the parasitic streaming flow would cause a convective heat leak on the hot heat exchanger lowering the efficiency of the TASHE. A detailed description of this phenomenon can be found elsewhere (Backhaus, 2000).

The TASHE is instrumented with many pressure sensors and type-K thermocouples. As shown in Fig. 1, the pressure sensors are located in the compliance, between the jet pump and cold heat exchanger, and at the junction between the inertance and TBT. A thermocouple is located in the center of the hot heat exchanger to measure the maximum hot end temperature, and a second is located on the outside diameter of the ambient heat exchanger. Several other thermocouples (not shown) are located throughout the TASHE to determine whether the temperature distribution in the important components are as predicted.

EFFICIENCY MEASUREMENTS

In these measurements, a resonator and variable acoustic load (Backhaus 2000, Fusco 1992) are used to mimic the lossless acoustic properties of a piston in a linear alternator, the parasitic losses due to piston motion, and the electrical load attached to the alternator. The length of the resonator is chosen so that the resonant frequency (frequency of operation) is ~88 Hz. This frequency is easily achievable with using currently available lightweight pistons. In all measurements, the center of the top plate of the TASHE hot heat exchanger is maintained at ~650 °C using a dc power supply, and the outer diameter of the ambient heat exchanger is maintained at ~25 °C by cooling water. The heater power is determined by simple current and voltage drop measurements. The pressure amplitude, which corresponds to piston stroke in a linear alternator, is varied by adjusting the variable acoustic load.

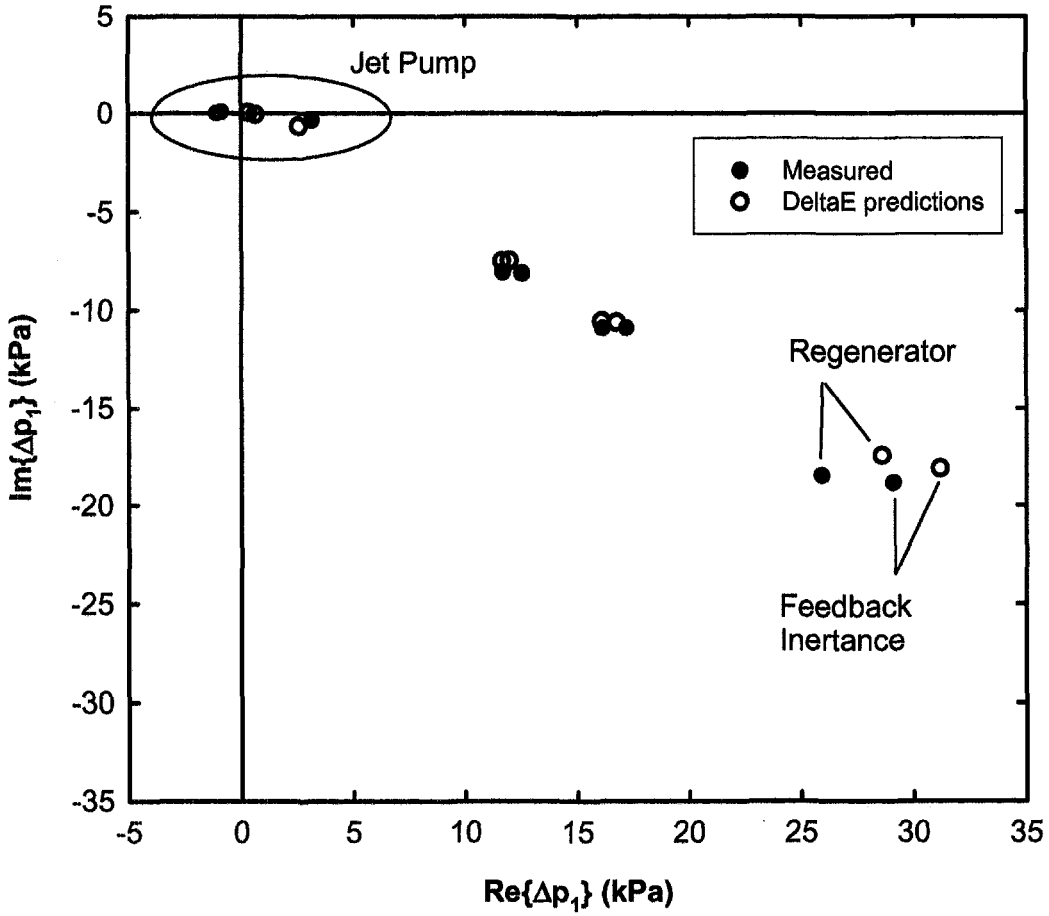

FIGURE 2. Pressure drops around the acoustic network. For clarity, points from three out of seven data sets are shown. The jet pump pressure drop is given by P1-P2, the regenerator pressure drop by P2-P3, and the feedback inertance drop by P1-P3 where P1 through P3 refer to locations in Fig. 1

First, the acoustic pressure drops across the various elements around the TASHE loop are measured. As shown in Fig. 2, the agreement between the measurements and numerical calculations using DeltaE (Ward 1994) are excellent implying that the numerical calculations are making accurate predictions of the acoustic velocities and the regenerator viscous pressure drop properties. This also implies that the calculation of the acoustic power circulating around the TASHE loop is accurate.

Figure 3 shows a comparison between the measured and predicted net high-temperature heat input and the acoustic power output at the alternator/resonator interface. Dc voltage and current measurements are used to determine the amount of heat delivered to the nickel heater block. A separate measurement is performed to determine how much of this heat leaks out through the insulation surrounding the hot heat exchanger. This heat leak is subtracted off of the total heat input to determine the net heat input to the TASHE's hot heat exchanger, which is presented in Fig. 3. The acoustic power is measured using a two-microphone technique; the measured amplitude and phase of the pressure at two locations in the resonator are used as inputs to a numerical calculation (Ward 1994) that determines the amount of power at the midpoint of the two sensors. When the acoustic flow is laminar, this technique agrees with an analytical calculation that assumes laminar flow (Fusco 1992). The numerical model is then used to extrapolate back to the resonator/alternator interface, and this power is presented in Fig. 3. The extra acoustic power added by the extrapolation is less than 17% of the total measured acoustic power in all cases.

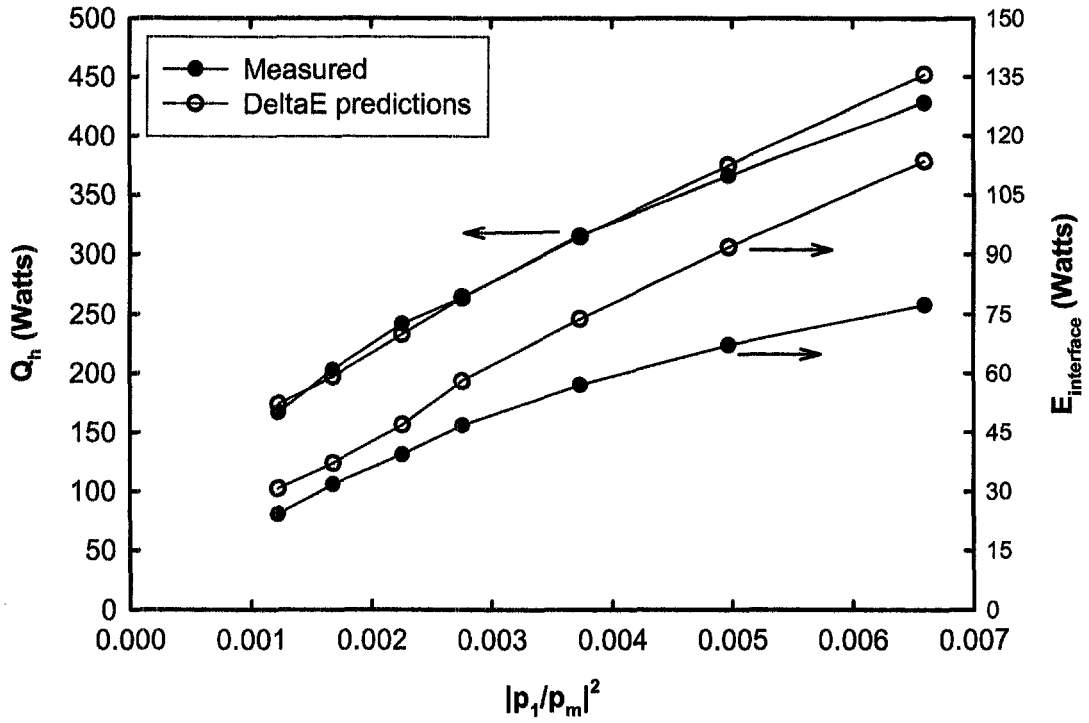

FIGURE 3. Net heat input and PV power output of the TASHE. The net heat input does not include thermal losses through the insulation surrounding the TASHE. As described in the text, the acoustic power at the resonator/alternator interface is extrapolated back from a measurement point in the resonator.

The excellent agreement between the measured and predicted heat input in Fig. 3 is not surprising given the agreement in Fig. 2. The net input to the TASHE is composed of the total power flowing into the TBT and back into the regenerator (Swift 2002). The total power into the TBT is mostly the acoustic power flowing away from the hot end of the regenerator. The agreement in Fig. 2 implies that this acoustic power is predicted well. The total power flowing back into the regenerator is due to enthalpy flux and relatively small metallic heat leaks (Swift 2002). The majority of the enthalpy flux is driven by the square of the acoustic velocity, which the data in Fig. 2 shows is well predicted. Therefore, good agreement between the measured and predicted heat input is expected. However, the discrepancy between the measured and predicted acoustic power at the interface is surprising.

The pressure-drop agreement in Fig. 2 and net heat input agreement in Fig. 3 provide evidence that the acoustic power circulating in the TASHE loop is as expected, but the acoustic power data in Fig. 3 show that there is less power delivered past the resonator/alternator interface than expected. One possibility is that there is an unaccounted for dissipation mechanism between the junction in Fig. 1 and the acoustic power measurement point farther down in the resonator. This seems unlikely since the geometry of the resonator between the two locations is quite simple; a straight duct. Another possibility, which has some experimental basis, is that the measurement technique is inaccurate. In all of our experimental set ups, the two-microphone technique is verified by varying the amount of power consumed by the variable acoustic load while maintaining a fixed pressure amplitude in the resonator (Backhaus 2000). All of the incremental power consumed by the load must pass through the two-microphone measurement point. In contrast to nearly all previous experimental setups, the present set up did not show all of the incremental power implying that the two-microphone acoustic power measurement is inaccurate. One possible reason for the discrepancy is that the acoustic flow in the resonator is highly turbulent.

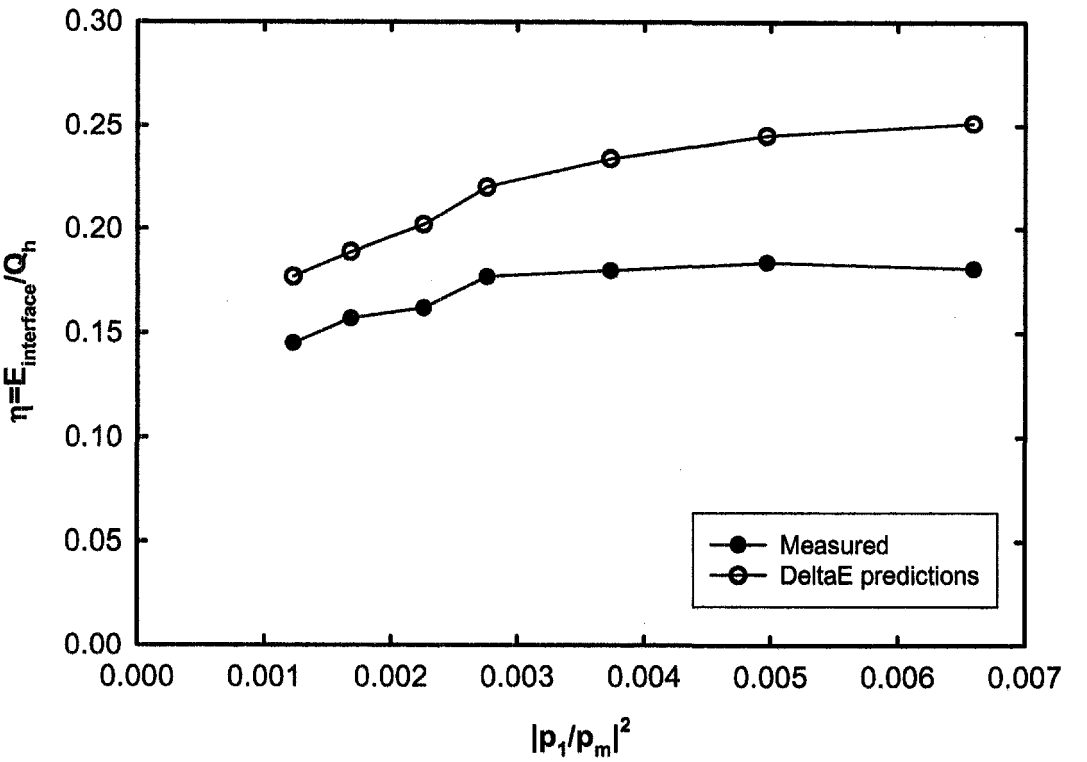

FIGURE 4. Thermal efficiency of the TASHE. The efficiency is based on the net heat input to the TASHE. The hot and cold end metal temperatures are maintained at 650 °C and 25 °C respectively. At the highest pressure amplitude, the TASHE would require a linear alternator with 27cc of swept volume.

When the conditions in the TASHE and resonator are modified to generate laminar flow, *e.g.* by lowering the static pressure and operating at low amplitude, both the analytical (Fusco 1992) and numerical (Ward 1994) method for calculating the two-microphone power agree with the incremental power into the acoustic load. When the flow is turbulent, both methods find less power passing the measurement point than is consumed in the acoustic load. The numerical technique, which attempts to account for turbulence (Ward 1994), is closer giving the known incremental acoustic power. Therefore, the acoustic power data presented in Fig. 3 is calculated using the numerical technique, but we believe the acoustic power delivered past the resonator/alternator interface is actually higher than the data points in Fig. 3.

Figure 4 presents the thermal efficiency of the TASHE, which is the ratio of the acoustic power delivered past the resonator/alternator interface to the net heat input to the TASHE hot heat exchanger. At the highest amplitude achieved, the efficiency is ~18% with 77 Watts of acoustic power delivered to the interface. The main reason for the discrepancy between the measured and predicted thermal efficiency is the deficit of acoustic power in Figure 3. Assuming a 90% efficient linear alternator, the overall system efficiency would be ~16% which is within the range desired by NASA (Mondt 2001). This efficiency is based on the acoustic power in Fig 3, which we believe is less than the actual power delivered by the TASHE. Future improvements, such as a parallel plate regenerator, will lead to efficiency improvements.

CONCLUSIONS

A thermoacoustic-Stirling heat engine (TASHE) has been successfully scaled down from the 1-kWatt range to the 100-Watt range while maintaining good thermal efficiency. The no-moving-parts TASHE allows for a flexible geometry that has resulted in a simple thermal interface to a GPHS. This flexibility will allow future designs to incorporate the ambient heat exchanger into the linear alternator itself simplify the remaining thermal interface.

Before current modifications, the TASHE demonstrated it is a low-mass power converter. At ~900 grams, it accounts less than 10% of the total mass of a 100-Watt-scale 10-Watt/kg power system.

ACKNOWLEDGMENTS

The authors would like to thank D. L. Gardner, C. Espinoza, M. Torres, and R. Haggart for their technical assistance in the construction of the TASHE. This work is funded by NASA under contract number NAS3-01103.

REFERENCES

Backhaus, S., and Swift, G. W., "A Thermoacoustic-Stirling Heat Engine: Detailed Study," Journal of the Acoustical Society of America, **107**, 3148-3166, 2000.

Backhaus, S., Tward, E., and Petach, M., "Thermoacoustic power systems for space applications," in proceedings of *Space Technology and Applications International Forum (STAIF-2001)* , edited by M. El-Genk, AIP Conference Proceedings 608, New York, 2001, pp. 939-944.

Fusco, A. M., Ward, W. C., and Swift, G. W., "Two-Sensor Power Measurements in Lossy Ducts," Journal of the Acoustical Society of America, **91**, 2229-2235, 1992.

Gedeon, D., "D. C. gas flows in Stirling and pulse-tube cryocoolers," *Cryocoolers 9*, edited by R. G. Ross, Plenum, New York, 1997, pp. 385-392.

Mondt, J. F., "Advanced Radioisotope Power System Technology Developments for NASA Missions 2001 and Beyond," Proceedings of the IECEC, 133-139, Savannah, GA, August, 2001.

Swift, G. W., "Thermoacoustics: A unifying perspective for some engines and refrigerators," Acoustical Society of America, 2002.

Tward, E., and Davis, T., "High Efficiency Cryocooler," AIAA, #99-4564, Albuquerque, NM, Sept. 1999.

Ward, W. C., and Swift, G. W., "Design Environment for Low Amplitude Thermoacoustic Engines, DeltaE," Journal of the Acoustical Society of America, **95**, 3671-3672, 1994. Fully tested software and users guide available from Energy Science and Technology Software Center, US Department of Energy, Oak Ridge, Tennessee. To review DeltaE's capabilities, visit the Los Alamos thermoacoustics web site at http://www.lanl.gov/projects/thermoacoustics/. For a beta-test version, contact ww@lanl.gov (Bill Ward) via Internet.